

## ON THE MESOSCOPIC MECHANISMS OF SPALL FRACTURE

Yu.I. Meshcheryakov, S.A. Atroshenko\*

Institute of Problems in Mechanical Engineering RAS, Saint Petersburg, 199178, Russia

\*e-mail: satroshe@mail.ru

**Abstract.** Four kinds of complex alloyed steel have been tested under uniaxial strain conditions within strain rate range of 215÷550 m/s. The kinematics of straining was studied by using SEM and optical microscopy of post-shocked specimens. The cross-section of targets is found to contain the mesoscopic rotational structures of complex configuration. Besides the free surface velocity, interference technique used allows the mean particle velocity profile and velocity variance to be registered in every shock loading. The spall strength is theoretically and experimentally found to be maximum at the strain rate where velocity variance equals to velocity defect. This condition means that local strain rate at the mesoscale equal to macroscopic strain rate. That strain rate corresponds to maximum density of rotations at the mesoscale.

**Keywords:** shock loading; spallation; rotational structures; velocity variance; velocity defect.

### 1. Introduction

In continuous mechanics, shock front is considered to be a particle velocity discontinuity, which means that all points of the front have identical particle velocities. In a multiscale mechanics, formation of shock front occurs owing to motion of elementary carriers of deformation at several scale levels including point defects, dislocations, mesoparticles and their combinations. As distinct from the quasistatics, where meso-particles are the concrete structural defects such as shear bands, rotational structures and other structural formations of scale 0.1-10  $\mu\text{m}$ , in the case dynamic deformation, the real carriers of deformation (point defects, dislocations, twins) cannot be identified. Concept of mesoparticle has a much wider meaning. In the latter case, the mesoparticles are the space structures the only specific feature of which is the *velocity correlated* motion of the mesovolumes. The only what can be estimated by using interference technique is the scale of correlated motion of elementary carriers of deformation. At the mesoscale this motion looks as a particle velocity pulsations. The scale of mesoparticle  $d_p$  is estimated to lie within interval  $\lambda_0 \ll d_p \ll L$ , where  $\lambda_0$  is the wave length of laser radiation and  $L$  is the diameter laser beam [1].

Shock-wave experiments [2-5], analytical studies [6] and molecular dynamics modeling [7] reveal specific features of shock-induced heterogenization of solids at the mesoscale. Specifically, propagation of shock front can be considered as a stochastic process. In simplest case, one can regard the motion of shock front in a heterogeneous medium as a superposition of two modes of motion: a mean motion which is a motion of approximately plane front, and rapidly fluctuating motion at the mesoscale about this mean motion due to action of local stress fields.

Modern shock-wave experiments show that shock wave propagation is characterized by two important features which cannot be taken into account for by the continuous mechanics: (i) propagation of shock front is a process which flows at the several scales; (ii) motion of shock front is non-uniform in the velocity space. It supposes that together with the average

particle velocity, there is a particle velocity distribution. In the case of structure-uniform material, the sufficient characteristic for the shock-wave process is a space-temporal velocity profile  $u_{fs}(t)$ . As for the heterogeneous material, the additional dynamic characteristic should be introduced - the particle velocity variance,  $D$  (square root of the particle velocity dispersion) [3,4]. Both characteristics can be determined by using the interference registration of shock-wave process. Typical free surface velocity profile for shock wave  $u_{fs}(t)$  and velocity variance profile  $D(t)$  in Cr-4Ni-Mo steel target are presented in Fig.1.

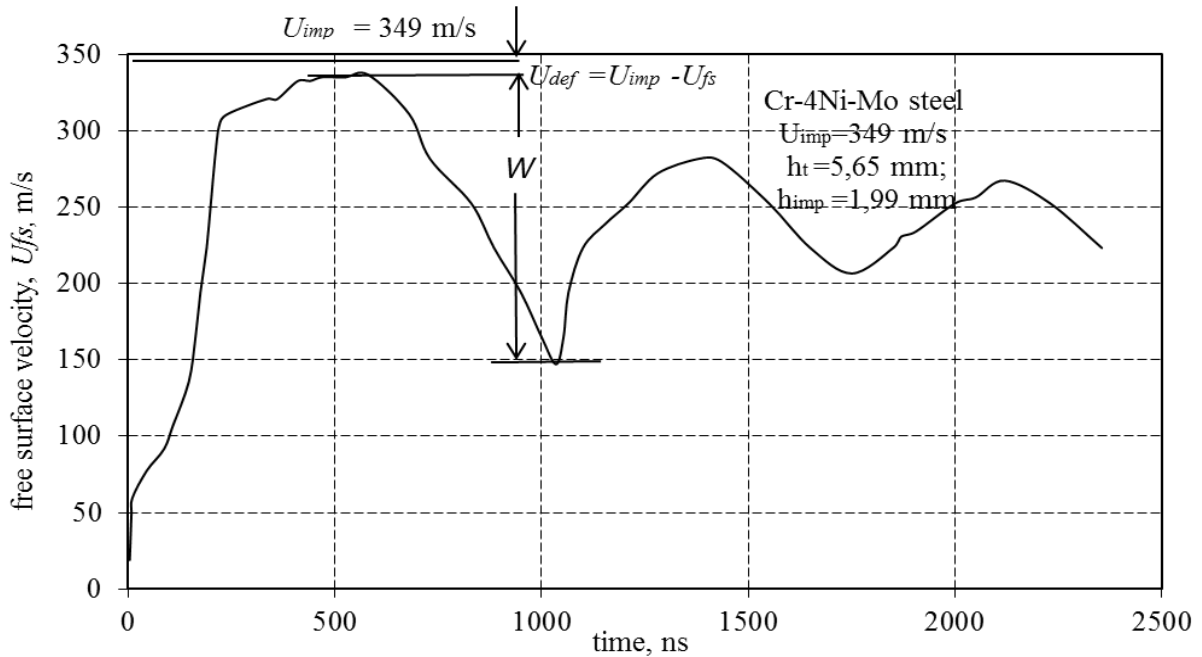


**Fig.1.** Free surface velocity profile,  $u_{fs}(t)$  and velocity variance,  $D(t)$ , for 5 mm Cr-4Ni-Mo steel target loaded at the impact velocity of 349 m/s.

The energy for swinging the velocity pulsations is taken from the external loading and is quantitatively characterized by the so-called "particle velocity defect"  $\Delta U_{def}$  which is determined as a difference between pick value of the free surface velocity at the plateau of compressive pulse  $u_{fs}^{max}$  and independently measured velocity of impactor under symmetrical collision, i.e. when acoustic impedances of impactor and target equal each other ( $\rho_{imp}C_{imp} = \rho_t C_t$ ):

$$\Delta U_{def} = U_{imp} - u_{fs}^{max} \quad (1)$$

The present paper provides the theoretical analysis and experimental results on shock loading for four kinds of high-strong complex alloyed steel which are typical examples of heterogeneous materials. The goal paper is to show how above dynamic characteristics – velocity variance,  $D$ , and velocity defect,  $\Delta U_{def}$  – provide a current coupling between mesoscale and macroscale of dynamic deformation and fracture and define the current dynamic strength of material.

## 2. Meso-macro energy exchange and spallation

The free surface profile characterizes a temporal history of mean particle velocity of dynamically deformed medium,

$$u(t) = \frac{1}{2} u_{fs}(t),$$

whereas the velocity variance,  $D(t)$  is a quantitative characteristics of scattering the particle velocity at the mesoscale (0.1-10  $\mu\text{m}$ ).

A following relationship between mean particle velocity  $u$ , velocity defect  $\Delta U_{def}$  and velocity variance,  $D$ , has been found [8]

$$\Delta U_{def} = -\frac{1}{2} \frac{d(D^2)}{dt} \quad (2)$$

This relationship provides a coupling between macroscale and mesoscale. It affirms that decrease (defect) of macroscopic particle velocity  $\Delta U_{def}$  is determined by the rate of change of the velocity variance in the velocity space. Eq. (2) can be written in the form

$$\Delta U_{def} = -D \frac{\frac{dD}{dt}}{\frac{du}{dt}} \quad (3)$$

If the rate of change of velocity variance equals to the rate of change of mean velocity

$$\frac{dD}{dt} = \frac{du}{dt}, \quad (4)$$

the velocity defect equals to the velocity variance

$$\Delta U_{def} = -D. \quad (5)$$

Eqs. (4) and (5) characterize an equilibrium regime of meso--macro energy exchange. In this case, the local deformation is determined by the displacements caused by the chaotic pulsations at the mesoscale. This situation closely determines the so-called Kolmogorov's universal regime in turbulence [9] where the steady regime of energy exchange supposes that interaction between turbulent pulsations is absent. In this case, all the space and temporal scales of the process are determined by the unit values of Reynolds number. In the case of dynamically deformed solid, this number links the velocity defect,  $\Delta U_{def}$ , scale of pulsations,  $L$ , and viscosity,  $\mu$  in the form:

$$\text{Re} = \frac{\Delta U_{def}}{\mu} L = 1 \quad (6)$$

The meso-macro energy exchange in form of (2-5) can be used to explain a non-monotonous behavior of spall strength depending on the strain rate. Structural investigation (see next section) show that spall zone of post-shocked targets contains a lot of chaotically distributed mesoscopic rotational formations. In this situation, one can suppose that shock wave energy coming to spall zone is spent on formation of rotational structures which are considered to be the basic kinematical mechanism of dynamic deformation for steels under consideration. The power balance at the spall zone can be written in the form:

$$\frac{1}{2} \rho C_0 u^2 = \frac{1}{2} \mu \frac{(u + \Delta U_{def})}{h} u + \frac{1}{2} \mu \frac{D}{h} u \quad (7)$$

Here  $\rho$  is a density of material,  $C_0$  is a velocity of shock wave,  $\mu$  is a dynamic viscosity of deformed material and  $u$  is the particle velocity. The left hand side item of Eq. (7) characterizes the power which is brought into spall zone from the load wave. The first item in the right hand side of equation describes the lost of power due to normal rupture of material under action of tension at the spall zone and reflects a motion of spall surfaces in opposite directions. The particle velocity is currently changes owing to meso-macro energy exchange

mechanism, so the mean particle velocity for this item includes the velocity defect  $\Delta U_{def}$ , and total strain rate at the spall zone due to normal tension equals:

$$\frac{d\varepsilon_1}{dt} = \frac{u + \Delta U_{def}}{h} \quad (8)$$

where  $h$  is the width of spall zone.

The conditions for continuity of deformed medium require that particle velocity distribution at the mesoscale inevitably causes the 3D motions of medium at that scale, i.e. local rotations.

The second item in the right hand side of Eq. (7) characterizes a power lost due to formation of rotation at the mesoscale at the strain rate

$$\frac{d\varepsilon_2}{dt} = \frac{D}{h}$$

From Eq. (7) the spall width  $h$  can be written in the form:

$$h = \left( \frac{\rho}{\mu} C_0 - \frac{\Delta U_{def} + D}{h} \frac{1}{u} \right)^{-1}. \quad (9)$$

Time for spallation can be defined as

$$\tau_f = \frac{h}{u} = \left( \sigma - \mu \frac{\Delta U_{def} + D}{h} \right)^{-1}, \quad (10)$$

where  $\sigma = \rho C_0 u$  is the normal stress in load wave. Eq. (10) can be rewritten in the form:

$$\left( \sigma - \mu \frac{\Delta U_{def} + D}{h} \right) \tau_f = 1. \quad (11)$$

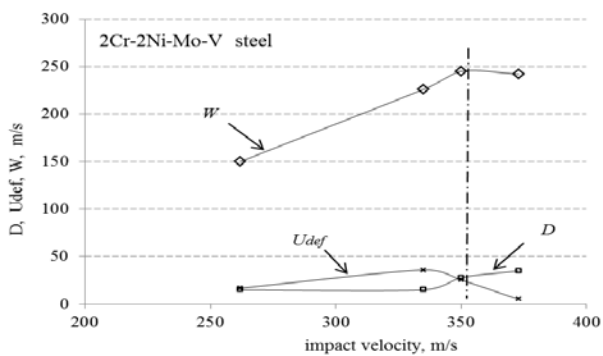
Dynamic generalization of this equation

$$\int_{t-\tau_f}^t \left( \sigma - \mu \frac{\Delta U_{def} + D}{h} \right) dt = 1 \quad (12)$$

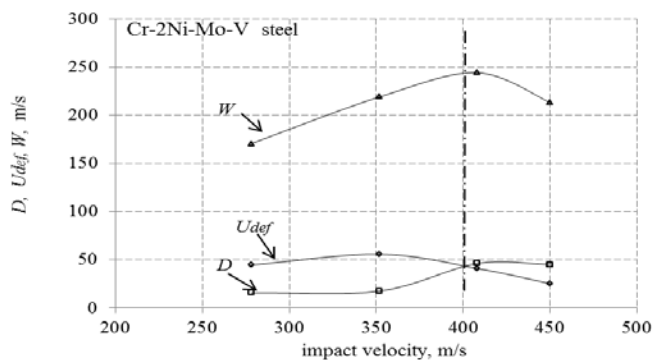
can be considered as a dynamic fracture criterion which takes into account both particle velocity distribution the mesoscale and the velocity defect resulting from meso-macro energy exchange. Being substituted into Eq. (12), condition (5) determines maximum value of normal stress necessary for dynamic fracture in accordance with integral criterion:

$$\int_{t-\tau_f}^t \sigma dt = 1. \quad (13)$$

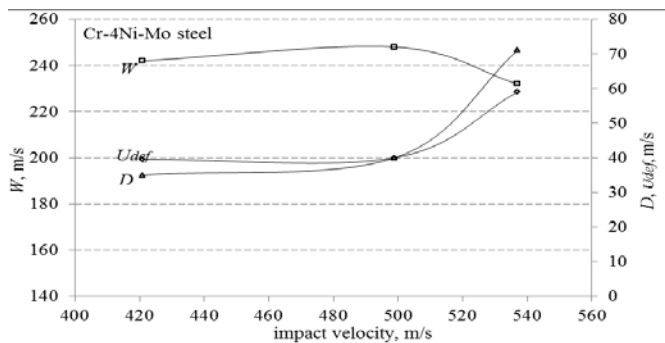
It is seen from Eq.(12) that maximum stress corresponds to equality  $\Delta U_{def} = -D$ .



a)



b)



c)

**Fig. 2.** Dependencies of pull-back velocity  $W$ , velocity defect,  $\Delta U_{def}$  and velocity variation,  $D$  on the impact velocity:  
 a) 2Cr-2Ni-Mo-V steel; b) Cr-2Ni-Mo-V steel; c) Cr-4Ni-Mo steel.

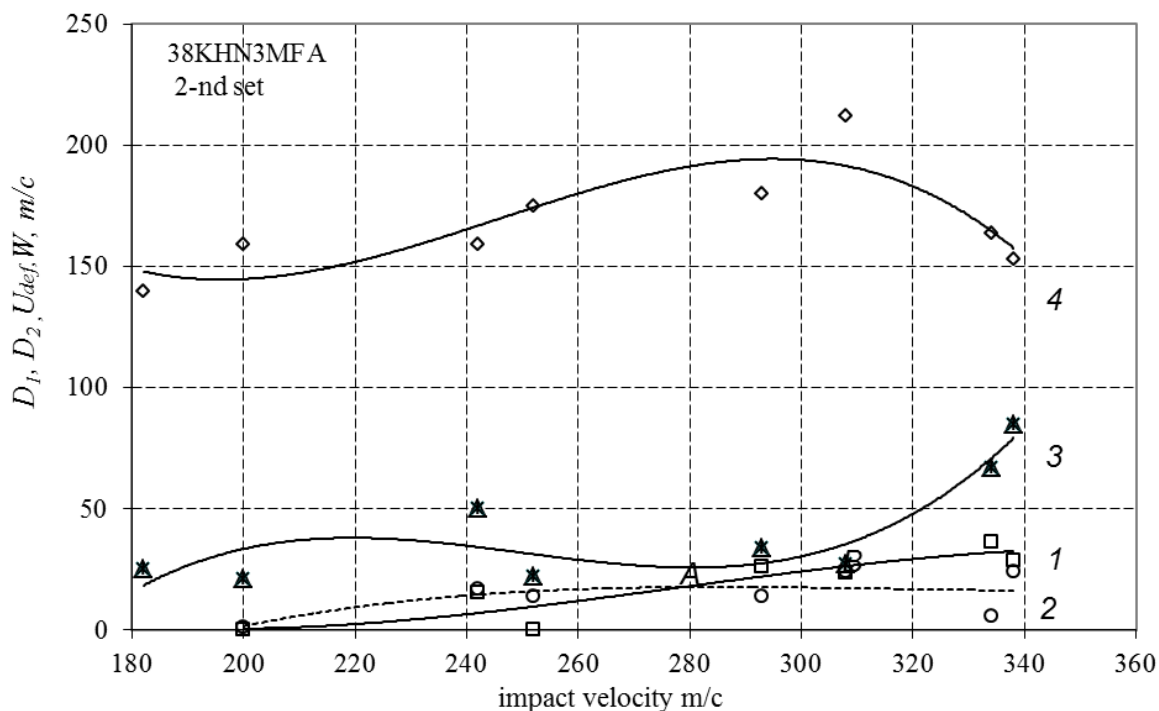


**Fig. 3.** Dependencies of velocity variance  $D$  (1), velocity defect  $\Delta U_{def}$  (2) and spall strength  $W$  (3) on the impact velocity for 38KHN3MFA steel.

Table 1. Chemical composition of steels.

Steel grade	Chemical composition, %							
	C	Si	Mn	Cr	Ni	Mo	V	Fe
2Cr-2Ni-Mo-V	0,3	0,25	0,45	1,7	1,7	0,8	0,12	rest
Cr-2Ni-Mo-V	0,34	0,2	0,4	1,3	1,7	0,85	0,13	
Cr-4Ni-Mo	0,3	0,2	0,4	1,3	3,7	0,8	-	

Table 2. Heat treatment of steels.

Steel grade	Heat treatment	Hardness
2Cr-2Ni-Mo-V	$t_{qI}=950^{\circ}\text{C}$ , 2h. + $t_t=625^{\circ}\text{C}$ , 4h. + $t_{qII}=825^{\circ}\text{C}$ , 2h. + $t_t=590^{\circ}\text{C}$ , 2h.	398 HB
Cr-2Ni-Mo-V	$t_{air\ q}=900^{\circ}\text{C}$ , 3h. + $t_{qII}=825^{\circ}\text{C}$ , 3h. + $t_t=590^{\circ}\text{C}$ , 4h.	388 HB
Cr-4Ni-Mo	$t_q=900^{\circ}\text{C}$ , 3h. + $t_t=550^{\circ}\text{C}$ , 3h.	39 HRC

where  $t_q$  – quenching temperature,  $t_t$  – tempering temperature,  $t_{air\ q}$  – air quenching.

Table 3. Pull-back velocity and rotations number.

Steel grade	$U_{imp}$	$W_{sp}$	$N_r$
2Cr-2Ni-Mo-V	262	150	
	335	225	
	350	245	
	373	241,8	
Cr-2Ni-Mo-V	278	197,5	145
	376	235	270
	423	245	119
	450	213,1	23

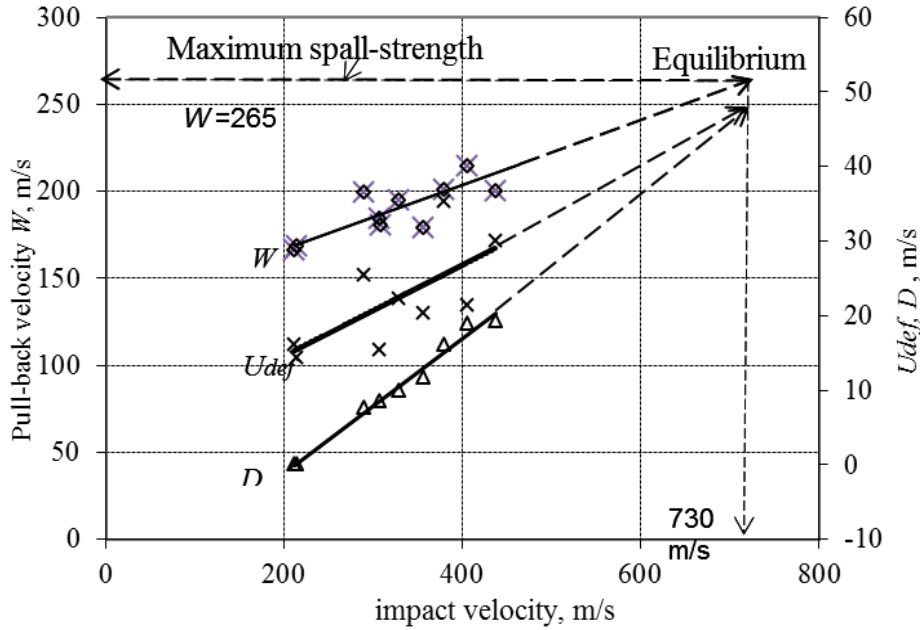


**Fig. 4.** Families of dependencies for the velocity variance,  $D$ , velocity defect  $\Delta U$ , and pull-back velocity  $W$ .

### 3. Experimental technique, materials and results of tests

Shock loading of targets under uniaxial strain conditions within impact velocities of 215–550 m/s, were carried out by using a one stage light gas gun of 37mm bore diameter. In the majority of tests, the impactor thickness was taken to provide spallation. Registration of the free surface velocity was performed by using two-channel velocity interferometer [1]. Besides the free surface velocity profiles,  $u_{fs}(t)$ , this interferometer allows the variance of the particle velocity at the mesoscale to be registered in real time. By using this technique, the shock-wave tests for four kinds of complex alloyed steel were performed. Chemical composition and regimes of heat treatment for the steels are provided in Tables 1 and 2, respectively. The results of testing are presented in Fig.2 (a-c) and Fig.3. Each figure presents three curves – velocity variance,  $D = f(U_{imp})$ , velocity defect  $\Delta U_{def} = f(U_{imp})$  and pull-back velocity  $W_{pb} = f(U_{imp})$  as functions of impact velocity.

The pull-back dependencies  $W$  as a measure of spall strength of material, show the maximum value just at the impact velocities where condition (5) is satisfied. From the physical point of view, maximum spall strength means that relaxation of internal stresses and meso-macro energy exchange flow in the most effective manner when strain rate at the mesoscale coincides with the macroscopic strain rate.

In special series of shock tests of Cr-4Ni-Mo steel targets within impact velocity range of 215- 550 m/s, three families of data – (i) particle velocity variance,  $D$ , (ii) velocity defect,  $\Delta U_{def}$ , and (iii) pull-back velocity,  $W$  - have been registered simultaneously (see Fig.4). After extrapolating the dependencies to higher impact velocities of the order of 730 m/s where they cross each other, it becomes evident that optimum impact velocity for this material corresponds to pull-back velocity of  $\sim 270$  m/s, i.e.  $\sim 25\%$  higher. This result has been checked in special experiment when analogous target has been shocked at the impact velocity of  $\sim 700$  m/s. The pull-back velocity turned out to be  $\sim 265$  m/s. These results allow the optimum regimes of application of steels to be determined after testing under uniaxial strain conditions with simultaneous registering the particle velocity variance, velocity defect and pull-back velocity.



**Fig.5.** Micrograph of elementary cell in the form of fan.

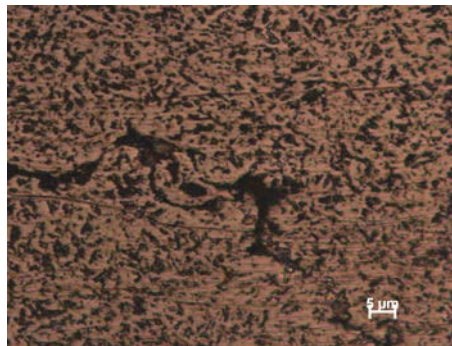


**Fig. 6.** Rotational spall split in steel Cr-2Ni-Mo-V.

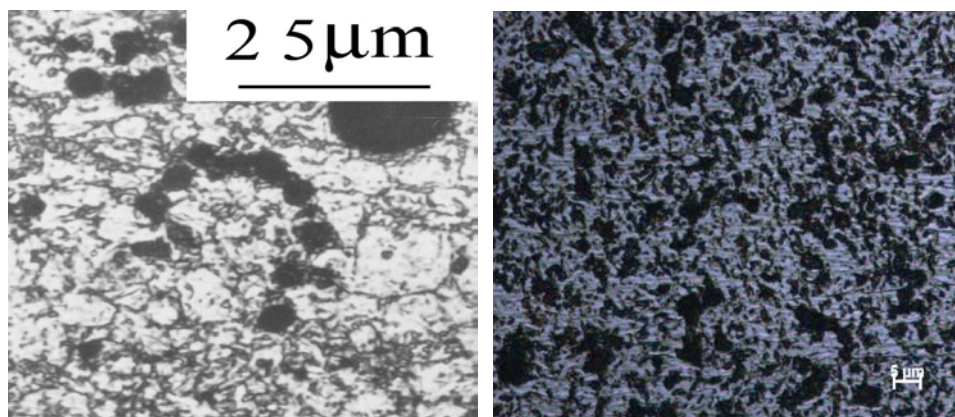


**Fig. 7.** Chain of rotational cells in the form of spirals and groups for Cr-4Ni-Mo steel (left) and for Cr-2Ni-Mo-V steel (right).

#### 4. Microstructure investigations

In order to reveal the mechanisms of dynamic deformation and fracture, the post-shocked targets were investigated using SEM and optical microscopy. The investigations confirm the 3D character of space morphology of carriers of deformation at the mesoscale. The distinct feature of steels under investigation is the rotational mechanism of dynamic straining. Rotational cells are complex formations which have been composed during the heat treatment of materials. Every rotational cell consists of central core of  $1\div 2\ \mu\text{m}$  in diameter and family of plates surrounding the core, so the rotational cell looks as fan of  $6\div 7\ \mu\text{m}$  in size. Chemical analysis performed using "Camscan" microscope shows that central core of cell (see Fig.5) is a harden carbide phase whereas surrounding plates are the martensite. Micrograph of rotational cell in steel target presented in Fig.6 and Fig.7 shows rotational spall split.

The rotational cells unite into chains, rings and spirals of  $50\div 100\ \mu\text{m}$  in size as shown in Fig. 6. Specifically, the spiral visualizes the eddy structure which has been formed under joint action of spherical component of tension stress and shear stress at the spall zone. Herewith, the rotational cells play a role of carriers of deformation at the mesoscale. Total length of spiral equals  $60\ \mu\text{m}$  while the duration of tension phase of stress at the spall zone  $\sim 0,3\ \mu\text{s}$ . From here the velocity of propagation of deformation front along the spiral equals  $\sim 200\ \text{m/s}$ , which is comparable to velocity of propagation of cracks in brittle materials.

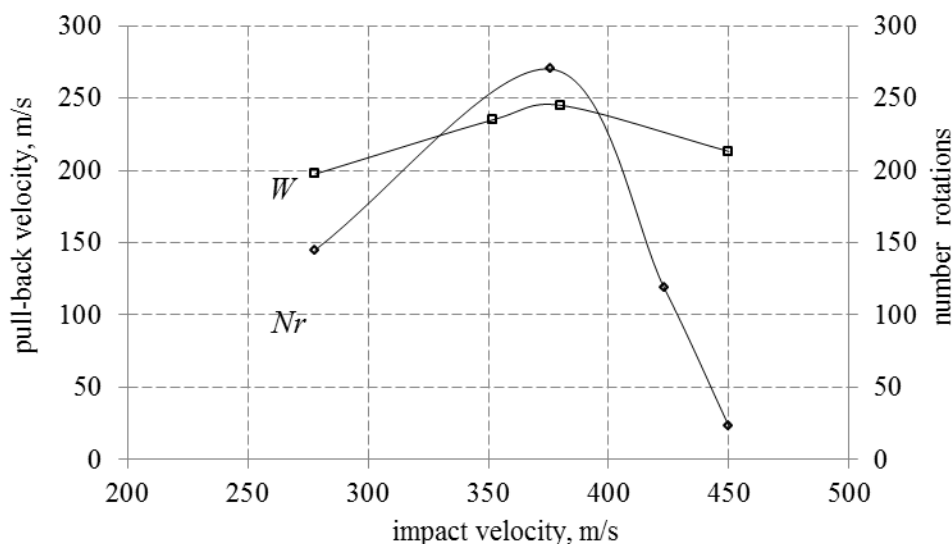


**Fig. 8.** Dependencies of pull-back-velocity,  $W$ , and number of rotational cells on the impact velocity for 2Cr-2Ni-Mo-V steel.

In Table 3 and Fig. 8 the values of pull-back velocity  $W$  and density of rotational cells depending on impact velocity are presented in parallel. The maximum spall strength is seen to corresponds to maximum density of rotational cells. This means that rotational mechanism of dynamic plasticity provides the most effective relaxation of internal stresses.

## 5. Conclusions

Shock tests of three kinds of complex alloyed steels reveal the following features of dynamic response on shock loading:

1. Maximum dynamic strength is shown to be realized at the strain rate where particle velocity variance (square root of the particle velocity dispersion) at the mesoscale equals to velocity defect at the plateau of compressive pulse.

2. Microstructure investigation of post-shocked targets shows that basic carriers of deformation at the mesoscale are the rotational cells which have a complex space morphology similar to fan construction - each rotational cell consists of central core of carbide phase and surrounding martensitic plates. In the process of dynamic straining, under action of stress field, a motion of martensitic plates around the central core is realized.

3. Maximum spall strength for all the tested steels corresponds to maximum density of rotational cells at the spall zone.

## References

- [1] Yu.I. Mescheryakov and A.K. Divakov // *Dymat Journal* **1(1)** (1994) 271.
- [2] J.R. Asay, L.C. Chhabildas, In: *Shock Waves and High-Strain Rate Phenomena in Metals*, ed. by M.A. Meyers and L.E. Murr (Plenum Publishing Co., N.Y., 1981), p.417.

- [3] Yu.I. Meshcheryakov, A.K. Divakov, N.I. Zhigacheva, I.P. Makarevich, B.K. Barakhtin // *Physical Review B* **78** (2008) 64301.
- [4] Yu.I. Meshcheryakov, A.K. Divakov, N.I. Zhigacheva // *Int. J. Solids and Structures* **41** (2004) 2349.
- [5] A.C. Koskelo, S.R. Greenfield, D.L. Raisley, K.J. McClellan, D.D. Byler, R.M. Dickerson, S.N. Luo, D.C. Swift, D.L. Tonk, P.D. Peralta, In: *Shock Compression of Condensed Matter -2007*. Proc. AIP-955 557-560 (2008).
- [6] D.E. Grady and M.E. Kipp // *J. Mech. Phys. Solids* **35(1)** (1987) 95.
- [7] K. Yano and Y-Y. Horie // *Physical Review B* **59** (1999) 103.
- [8] Yu.I. Meshcheryakov, In: *High-Pressure Shock Compression of Solids VI*, ed. by Y-Y. Horie, L. Davison, N.N. Thadhani (Springer, 2002), p.169.
- [9] J.O. Hinze // *Turbulence* (Mc. Graw Hill Inc., New York. 1959), p.680.